



In-silico evaluation of approved drugs for possible blockade of sars-cov-2 spike glycoprotein interactions with angiotensin-converting enzyme 2

Ilomuanya Ifeanyi Evaristus¹, Okika Maureen Chidera², *Ejiofor Innocent Mary Ifedibaluchukwu³

¹Department of Pharmacy, Nnamdi Azikiwe University Teaching Hospital, Nnewi, Anambra State, Nigeria

²Department of Pharmacy, Federal Medical Centre, Onitsha, Anambra State, Nigeria

³Department of Pharmacognosy and Traditional Medicine, Faculty of Pharmaceutical Sciences, Nnamdi Azikiwe University, Awka, Anambra State, Nigeria.

Corresponding author: Ejiofor Innocent Mary Ifedibaluchukwu

Faculty of Pharmaceutical Sciences, Nnamdi Azikiwe University, Awka, Anambra State, Nigeria

ii.ejiofor@unizik.edu.ng

+2349011581000

Article History

Volume 6 Issue 12, 2024

Received: 25 May 2024

Accepted: 25 June 2024

doi:

10.48047/AFJBS.6.12.2024.1287-1302

Abstract

In late 2019, an outbreak of COVID-19 caused by SARS-COV-2 was declared a pandemic. The outbreak killed millions of people and caused economic instability in different countries due to movement restrictions. The pandemic may have ended, but there is a need to understand how to handle such cases better using already-approved molecules in the event of future occurrences. In this study, we utilized computational approaches to gain insight into the infestation mechanism of SARS-COV-2 and possible blockade with approved drugs. We obtained 2015 approved drugs from drugbank and representatives of the spike glycoprotein interaction with angiotensin-converting enzyme 2 (ACE2). We carried out sequence alignment of the spike glycoprotein of different SARS-COV-2 variants using clustal omega. We evaluated the amino acids involved in the viral attachment. We carried out molecular docking simulations in the selected interaction regions. Nine (9) interaction regions were found in the SARS-COV-2 spike bridge formation with ACE2. We undertook post docking and analysis and 2D visualization of selected docked complexes. The SARS-COV-2 spike glycoprotein variants were similar in the region of the spike protein interaction with the ACE2, except for the omicron variant. The top 20 frontrunner drugs on different interaction points were selected based on the mean values of the binding affinities obtained from molecular docking simulations. The visualization of top multitargeting drugs Dutasteride, Ergotamine, Folic acid, Piroxicam, Ketoconazole, Ceftriaxone, Amodiaquine and Methotrexate, revealed interactions that could possibly block SARS-COV-2 spike glycoprotein interaction with ACE2 receptor. Further studies will be carried out to observe the stability of the frontrunner complexes.

Keywords: SARS-COV-2, ACE2, Approved drugs, In-silico, spike glycoprotein

Introduction

In late 2019, a novel coronavirus emerged, rapidly transforming from a localized outbreak into a global pandemic known as COVID-19. Scientists swiftly identified the culprit as a new member of the beta coronavirus family, severe acute respiratory syndrome coronavirus 2 (SARS-CoV-2) [1,2]. While most human coronaviruses cause mild cold-like symptoms, SARS-CoV-2 joins a trio- including SARS-CoV and MERS-CoV with the potential for severe illness and death [2]. By Dec 31, 2021, global reported deaths due to COVID-19 reached 5.94 million, but the estimated number of excess deaths was nearly 3.07-times (95% UI 2.88–3.30) greater, reaching 18.2 million (17.1–19.6). The global all-age rate of excess mortality due to the COVID-19 pandemic was 120.3 deaths (113.1–129.3) per 100 000 of the population [3].

According to statistics [4], by mid-November 2022, Africa had recorded roughly 12.7 million COVID-19 cases. This accounted for only about 2% of global infections at that time. Worldwide, over 640 million people have contracted the virus, with more than 6 million sadly succumbing to it. However, there was a glimmer of hope - approximately 620 million individuals had recovered. South Africa bore the brunt of the pandemic on the continent, with infections exceeding 3.6 million.

The emergence of COVID-19 has triggered a global health crisis, but its impact extends far beyond. The virus unleashed an unprecedented economic threat, leaving many scrambling for solutions. The lack of readily available treatments and preventative measures paints a particularly concerning picture.

Developing entirely new drugs from scratch is a time-consuming and expensive process, often taking years to complete. In urgent situations, repurposing existing drugs offers a more efficient approach. By leveraging medications already approved for other uses, we can fast-track treatment options and reduce the financial burden of drug discovery. One of the main therapeutic targets against COVID-19 is the inhibition of spike protein, as it aids in both the recognition and binding of the virus to the host cell [5].

SARS-CoV-2, a single-stranded RNA virus, has a fully sequenced genome revealing its blueprint. This 30,000-base code encodes nearly 10,000 amino acids, the building blocks of viral proteins. Some proteins form the virus's outer shell, while others play crucial roles in its internal machinery [6].

A dense coat of sugars adorns the surface of SARS-CoV-2, specifically its spike (S) protein. This sugary facade allows the virus to latch onto a human cell receptor called angiotensin-converting enzyme 2 (ACE2) and gain entry into the cell. Once inside, the viral RNA is released and translated into proteins. These proteins then work together to replicate the viral genome and assemble new virus particles, ready for their release and the continuation of the infectious cycle [7,8].

During the COVID-19 pandemic, the wait for the development of a vaccine, the unavailability of COVID-19 treatment options and the rapid nature of the infection resulted in many casualties. Some already existing drugs were used for the management of COVID-19 symptoms in an attempt to reduce the mortality rate. Some of the therapeutic agents that have the potential against the spike protein are Ritonavir, Remdesivir, and Camostat, as well as Azithromycin and Chloroquine/Hydroxychloroquine. However, the potential needs to be proved and necessitates further clinical studies [9].

To ensure the safety of the global populace in future occurrences like the COVID-19 pandemic, there is a need to establish a possible and efficient guideline to immediately search for a treatment option from the approved drug molecules. In this study, we assessed, using in-silico

techniques, already existing and approved drug molecules for possible blockage of the interaction between COVID-19 spike glycoprotein and angiotensin-converting enzyme 2 (ACE2), which is essential for the entry of the COVID-19 virus into the human host.

Materials and Methods

Personal Computer with Linux operating system, 2015 approved drugs, Protein data bank (www.pdb.com), PubChem (<https://pubchem.ncbi.nlm.nih.gov>), Clustal Omega (<https://www.ebi.ac.uk/jdispatcher/msa/clustalo>), Ligplot [10], PyMol [11], Bash script for molecular docking simulation and Python scripts for the extraction of binding energy scores, Autodock tools 1.5.6, Autodock vina 1.1.2 [12,13], Biovia Discovery Studio Visualizer [14].

Literature Mining

Journal publications and biological databases were mined to identify essential interacting amino acid residues in the spike protein of SARS COV-2 variants, including the wild-type, beta, delta, gamma, and omicron variants.

Sequence alignment

The amino acid sequences of the COVID-19 wide type and variants were obtained from the protein data bank, with protein data bank codes 6VSB, 7VXD, 7V7Q, 7SBS and 7T9J for Alpha, Beta, Delta, Gamma, and Omicron variants, respectively. The sequences were aligned on the Clustal Omega web page. The alignment was done to identify the point of amino acid mutation of the variants compared to the wide type.

Identification of the interacting amino acid residues

With the aid of the Ligplot application, 2D models of the interactions between the spike protein of the COVID-19 virus and ACE2 were generated. It gives insights into the specific amino acids from the spike protein responsible for the bond formation with the amino acids of the ACE2.

Selection and preparation of the receptor

After the identification of several targets, literature mining and analysis, proper targets were selected: the Alpha variant (6vsb), the Beta variant (7vxd), the Delta variant (7v7q), the Gamma variant (7sbs) and the Omicron variant (7T9J). The 3D coordinates of the variants were obtained from the protein data bank and prepared for molecular docking simulation. The receptors were visualized and edited with PyMol. Water molecules were also removed. Polar hydrogens were added to receptors using Autodock tools. The grid boxes were called up, and appropriate xyz coordinates were chosen to cover the points of interactions between the spike protein and ACE2. The grid parameters were obtained and saved in a notepad as a configuration file. The receptors were saved as pdbqt files.

Selection and preparation of Ligands

The 2015 ligands (approved drugs) used in the molecular docking simulation were obtained from the Drug bank in the SDF format. The ligands were prepared using a bash script that enable energy minimization, was performed using the steepest descent minimization algorithm with General Amber Force Field on the Open Babel application, and the SDF file formats were converted to pdbqt.

Molecular Docking Simulations

A molecular docking simulation between the receptors and the ligands was executed in triplicate on Autodock_vina using a bash script that automates molecular docking on the Linux operating system.

Post-Docking analysis

The results obtained from the docked ligands were extracted using Python script and copied and pasted into the MS Excel spreadsheets. The results were then sorted and filtered to determine the

ligands with the higher binding affinities. The means and standard deviations of the binding affinity scores were calculated.

Ligands with higher binding affinities were selected and visualized using the Biovia Discovery Studio visualizer to observe for possible interactions of the ligands at the interface between the spike protein of the Covid-19 virus and human ACE2.

Results and discussions

Covid-19 virus spike glycoprotein-ACE2 interface

Represented in Figure 1 below is the COVID-19 virus spike glycoprotein-ACE2 interface as obtained from the Protein data bank. The blue part represents the spike glycoprotein, while the green represents the ACE2 receptor. A key to tackling this pandemic is to understand the receptor recognition mechanism of the virus, which regulates its infectivity, pathogenesis and host range. SARS-CoV-2 and SARS-CoV recognize the same receptor-angiotensin-converting enzyme 2 (ACE2)-in humans [15, 16]. The crystal structure of the receptor-binding domain (RBD) of the spike protein of SARS-CoV-2 in a complex with ACE2 guides intervention strategies that target receptor recognition by SARS-CoV-2 [17]. Since this interaction is necessary for the infectivity of the virus to the human host, bridging this interaction or its disruption may cause viral penetration unease.

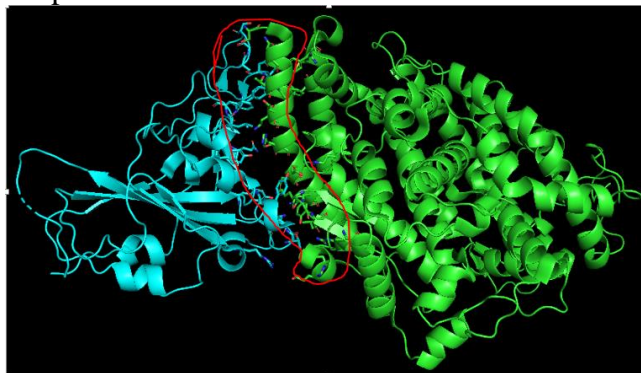


Figure 1: Covid-19 virus spike glycoprotein-ACE2 interface

Sequence alignment

The multiple sequence alignment of the spike glycoprotein from different SAR-COV2 variants is present in Figure 2 below. The sequence shows the residues of similarity and difference among the sequences. Multiple sequence alignment (MSA) has assumed a vital role in biological sequences' comparative structure and function analysis. It often leads to fundamental biological insight into sequence-structure-function relationships of nucleotide or protein sequence families [18]. Mutation change or deletion of amino acid residue(s) can lead to the ineffectiveness of drug molecules. It has long been recognized that mutations and variations in amino acids play a significant role as hereditary factors in human disorders. Protein expression and subcellular localization [19,20], protein function [21,22], protein-protein interactions [23-26], and protein folding and stability [27-32] can all be impacted by mutations. This study's alignment helped us observe if the interacting residues of spike glycoproteins from the variants are the same. Any mutation that affects the interacting residues will probably affect the drug's effectiveness at the Covid-19 virus spike glycoprotein-ACE2 interface. In Figure 2, * represents the same residue.. and : represent points of variations while gaps represent deletion of amino acid residues.

CLUSTAL 0(1.2.4) multiple sequence alignment		7SBS_1 Chains	7SBS_1 Chains
7SBS_1 Chains	MFVFLVLLPLVSSQCVNLTTRTQLPPAYTNSFTRGVYYPDKVFRSSVLHSTQDLFLPFFS	7V7Q_1 Chains	GKQGNFKNLSEFVKNIQGYFKIYSKHTPINL--VRDLPGQSALEPLVDLPIGINITRF
7V7Q_1 Chains	MFVFLVLLPLVSSQCVNLTTRTQLPPAYTNSFTRGVYYPDKVFRSSVLHSTQDLFLPFFS	7V7Q_1 Chains	GKQGNFKNLREFVFKNIQGYFKIYSKHTPINL--VRDLPGQSALEPLVDLPIGINITRF
7T9J_1 Chains	MFVFLVLLPLVSSQCVNLTTRTQLPPAYTNSFTRGVYYPDKVFRSSVLHSTQDLFLPFFS	7T9J_1 Chains	GKQGNFKNLREFVFKNIQGYFKIYSKHTPIVREPDLPGQSALEPLVDLPIGINITRF
6VSB_1 Chains	MFVFLVLLPLVSSQCVNLTTRTQLPPAYTNSFTRGVYYPDKVFRSSVLHSTQDLFLPFFS	6VSB_1 Chains	GKQGNFKNLREFVFKNIQGYFKIYSKHTPINL--VRDLPGQSALEPLVDLPIGINITRF
7VXD_1 Chains	MFVFLVLLPLVSSQCVNLTTRTQLPPAYTNSFTRGVYYPDKVFRSSVLHSTQDLFLPFFS	7VXD_1 Chains	GKQGNFKNLREFVFKNIQGYFKIYSKHTPINL--VRDLPGQSALEPLVDLPIGINITRF
	*****: .*****		*****: .*****
7SBS_1 Chains	NVTFWFAIHVSGTNGTKRFNDPVLFPNDGVYFASTEKSNIRGWIFGTTLDSKQSLLV	7SBS_1 Chains	QTLALHRSYLTGPDSSSGWTAGAAAYVGYLQPRFLLKYNGENTITDAVDCALDPLSE
7V7Q_1 Chains	NVTFWFAIHVSGTNGTKRFNDPVLFPNDGVYFASTEKSNIRGWIFGTTLDSKQSLLV	7V7Q_1 Chains	QTLALHRSYLTGPDSSSGWTAGAAAYVGYLQPRFLLKYNGENTITDAVDCALDPLSE
7T9J_1 Chains	NVTFWFAIHVSGTNGTKRFNDPVLFPNDGVYFASTEKSNIRGWIFGTTLDSKQSLLV	7T9J_1 Chains	QTLALHRSYLTGPDSSSGWTAGAAAYVGYLQPRFLLKYNGENTITDAVDCALDPLSE
6VSB_1 Chains	NVTFWFAIHVSGTNGTKRFNDPVLFPNDGVYFASTEKSNIRGWIFGTTLDSKQSLLV	6VSB_1 Chains	QTLALHRSYLTGPDSSSGWTAGAAAYVGYLQPRFLLKYNGENTITDAVDCALDPLSE
7VXD_1 Chains	NVTFWFAIHVSGTNGTKRFNDPVLFPNDGVYFASTEKSNIRGWIFGTTLDSKQSLLV	7VXD_1 Chains	QTLALHRSYLTGPDSSSGWTAGAAAYVGYLQPRFLLKYNGENTITDAVDCALDPLSE
	***** * *****		** * *****
7SBS_1 Chains	NNATNVVIVKCEFCNDPFLGVYHKNKSWMESEFRVYSSANCTFEVYSPFLMDLE	7SBS_1 Chains	TKCTLKSFTEKGIYQTSNFRVQPTESIVRFPNITLCPFGVEFNATRFASVYAMNRKRI
7V7Q_1 Chains	NNATNVVIVKCEFCNDPFLGVYHKNKSWMESEFRVYSSANCTFEVYSPFLMDLE	7V7Q_1 Chains	TKCTLKSFTEKGIYQTSNFRVQPTESIVRFPNITLCPFGVEFNATRFASVYAMNRKRI
7T9J_1 Chains	NNATNVVIVKCEFCNDPFLGVYHKNKSWMESEFRVYSSANCTFEVYSPFLMDLE	7T9J_1 Chains	TKCTLKSFTEKGIYQTSNFRVQPTESIVRFPNITLCPFGVEFNATRFASVYAMNRKRI
6VSB_1 Chains	NNATNVVIVKCEFCNDPFLGVYHKNKSWMESEFRVYSSANCTFEVYSPFLMDLE	6VSB_1 Chains	TKCTLKSFTEKGIYQTSNFRVQPTESIVRFPNITLCPFGVEFNATRFASVYAMNRKRI
7VXD_1 Chains	NNATNVVIVKCEFCNDPFLGVYHKNKSWMESEFRVYSSANCTFEVYSPFLMDLE	7VXD_1 Chains	TKCTLKSFTEKGIYQTSNFRVQPTESIVRFPNITLCPFGVEFNATRFASVYAMNRKRI
	***** *		***** *
7SBS_1 Chains	SNCVADSVLYNSASFSTFKCYGVSPTKLNLDLCTNVAADSVIRGDEVRIAPGQTGTI	7SBS_1 Chains	VNFNFLGTGTVLSTESNKKFLPFQGFGRDIAOTDVAVRDPTLEIDITPCSFGGVSVI
7V7Q_1 Chains	SNCVADSVLYNSASFSTFKCYGVSPTKLNLDLCTNVAADSVIRGDEVRIAPGQTGTI	7V7Q_1 Chains	VNFNFLGTGTVLSTESNKKFLPFQGFGRDIAOTDVAVRDPTLEIDITPCSFGGVSVI
7T9J_1 Chains	SNCVADSVLYNLAPFFTKCYGVSPTKLNLDLCTNVAADSVIRGDEVRIAPGQTGTI	7T9J_1 Chains	VNFNFLGTGTVLSTESNKKFLPFQGFGRDIAOTDVAVRDPTLEIDITPCSFGGVSVI
6VSB_1 Chains	SNCVADSVLYNSASFSTFKCYGVSPTKLNLDLCTNVAADSVIRGDEVRIAPGQTGTI	6VSB_1 Chains	VNFNFLGTGTVLSTESNKKFLPFQGFGRDIAOTDVAVRDPTLEIDITPCSFGGVSVI
7VXD_1 Chains	SNCVADSVLYNSASFSTFKCYGVSPTKLNLDLCTNVAADSVIRGDEVRIAPGQTGTI	7VXD_1 Chains	VNFNFLGTGTVLSTESNKKFLPFQGFGRDIAOTDVAVRDPTLEIDITPCSFGGVSVI
	***** * *****		***** * *****
7SBS_1 Chains	ADYNYKLPDDFTGCVIAMSNNLDSKVGGNVYLYRFRKSNLKPFFRISTEIQAGST	7SBS_1 Chains	TPGNTSNQVAVLYQGVNCTEVPVAIHADQLPTWRVYSTGSMVFQTRAGLIGAEVNN
7V7Q_1 Chains	ADYNYKLPDDFTGCVIAMSNNLDSKVGGNVYLYRFRKSNLKPFFRISTEIQAGST	7V7Q_1 Chains	TPGNTSNQVAVLYQGVNCTEVPVAIHADQLPTWRVYSTGSMVFQTRAGLIGAEVNN
7T9J_1 Chains	ADYNYKLPDDFTGCVIAMSNNLDSKVGGNVYLYRFRKSNLKPFFRISTEIQAGST	7T9J_1 Chains	TPGNTSNQVAVLYQGVNCTEVPVAIHADQLPTWRVYSTGSMVFQTRAGLIGAEVNN
6VSB_1 Chains	ADYNYKLPDDFTGCVIAMSNNLDSKVGGNVYLYRFRKSNLKPFFRISTEIQAGST	6VSB_1 Chains	TPGNTSNQVAVLYQGVNCTEVPVAIHADQLPTWRVYSTGSMVFQTRAGLIGAEVNN
7VXD_1 Chains	ADYNYKLPDDFTGCVIAMSNNLDSKVGGNVYLYRFRKSNLKPFFRISTEIQAGST	7VXD_1 Chains	TPGNTSNQVAVLYQGVNCTEVPVAIHADQLPTWRVYSTGSMVFQTRAGLIGAEVNN
	***** * *****		***** * *****
7SBS_1 Chains	PCNGVGFNCYFPLQSYGFOPTNGVGYQYRNVVLSFELLHAPATVCGPKKSTNLVKNK	7SBS_1 Chains	SYECDPIGAGICASYQTQNSRRARSVASQSIAYTMSLGAENSVAYSNNSIAIPTNF
7V7Q_1 Chains	PCNGVGFNCYFPLQSYGFOPTNGVGYQYRNVVLSFELLHAPATVCGPKKSTNLVKNK	7V7Q_1 Chains	SYECDPIGAGICASYQTQNSRRARSVASQSIAYTMSLGAENSVAYSNNSIAIPTNF
7T9J_1 Chains	PCNGVGFNCYFPLQSYGFOPTNGVGYQYRNVVLSFELLHAPATVCGPKKSTNLVKNK	7T9J_1 Chains	SYECDPIGAGICASYQTQNSRRARSVASQSIAYTMSLGAENSVAYSNNSIAIPTNF
6VSB_1 Chains	PCNGVGFNCYFPLQSYGFOPTNGVGYQYRNVVLSFELLHAPATVCGPKKSTNLVKNK	6VSB_1 Chains	SYECDPIGAGICASYQTQNSRRARSVASQSIAYTMSLGAENSVAYSNNSIAIPTNF
7VXD_1 Chains	PCNGVGFNCYFPLQSYGFOPTNGVGYQYRNVVLSFELLHAPATVCGPKKSTNLVKNK	7VXD_1 Chains	SYECDPIGAGICASYQTQNSRRARSVASQSIAYTMSLGAENSVAYSNNSIAIPTNF
	***** * *****		***** * *****
7SBS_1 Chains	TISVTEILPVSMTKTSVDCMYICGDSSTECNLLQYGSFCTQLNRALTGIAVEQDKNT	7SBS_1 Chains	AMQMAYRFNGIGVTVNLYENQKLIANQFNSAIGIKQDLSSTASALGKLDVWNQNAQA
7V7Q_1 Chains	TISVTEILPVSMTKTSVDCMYICGDSSTECNLLQYGSFCTQLNRALTGIAVEQDKNT	7V7Q_1 Chains	AMQMAYRFNGIGVTVNLYENQKLIANQFNSAIGIKQDLSSTASALGKLDVWNQNAQA
7T9J_1 Chains	TISVTEILPVSMTKTSVDCMYICGDSSTECNLLQYGSFCTQLNRALTGIAVEQDKNT	7T9J_1 Chains	AMQMAYRFNGIGVTVNLYENQKLIANQFNSAIGIKQDLSSTASALGKLDVWNQNAQA
6VSB_1 Chains	TISVTEILPVSMTKTSVDCMYICGDSSTECNLLQYGSFCTQLNRALTGIAVEQDKNT	6VSB_1 Chains	AMQMAYRFNGIGVTVNLYENQKLIANQFNSAIGIKQDLSSTASALGKLDVWNQNAQA
7VXD_1 Chains	TISVTEILPVSMTKTSVDCMYICGDSSTECNLLQYGSFCTQLNRALTGIAVEQDKNT	7VXD_1 Chains	AMQMAYRFNGIGVTVNLYENQKLIANQFNSAIGIKQDLSSTASALGKLDVWNQNAQA
	***** * *****		***** * *****
7SBS_1 Chains	QEVFAQVQIYKTPPIKDFGGFNFSQILPDPKSPKRSFIEDLLFNKVTADAGFIQYG	7SBS_1 Chains	LNTLVKQLSSNFGAISSVLNDILSRDLKPEAEVQIDRLITGRQLSQTQVTVQQLIRAAEI
7V7Q_1 Chains	QEVFAQVQIYKTPPIKDFGGFNFSQILPDPKSPKRSFIEDLLFNKVTADAGFIQYG	7V7Q_1 Chains	LNTLVKQLSSNFGAISSVLNDILSRDLKPEAEVQIDRLITGRQLSQTQVTVQQLIRAAEI
7T9J_1 Chains	QEVFAQVQIYKTPPIKDFGGFNFSQILPDPKSPKRSFIEDLLFNKVTADAGFIQYG	7T9J_1 Chains	LNTLVKQLSSNFGAISSVLNDILSRDLKPEAEVQIDRLITGRQLSQTQVTVQQLIRAAEI
6VSB_1 Chains	QEVFAQVQIYKTPPIKDFGGFNFSQILPDPKSPKRSFIEDLLFNKVTADAGFIQYG	6VSB_1 Chains	LNTLVKQLSSNFGAISSVLNDILSRDLKPEAEVQIDRLITGRQLSQTQVTVQQLIRAAEI
7VXD_1 Chains	QEVFAQVQIYKTPPIKDFGGFNFSQILPDPKSPKRSFIEDLLFNKVTADAGFIQYG	7VXD_1 Chains	LNTLVKQLSSNFGAISSVLNDILSRDLKPEAEVQIDRLITGRQLSQTQVTVQQLIRAAEI
	***** * *****		***** * *****
7SBS_1 Chains	DCLGDI AARDLICAQKFNGLTVLPLLLTDEMI AQYTSALLAGTITSGWTFGAGAALQIPF	7SBS_1 Chains	RASANLAATKMSCEVLGQSKRVDFCGKGYHLSMFPQSAHPGVVFLHVTYVPAQENFTTA
7V7Q_1 Chains	DCLGDI AARDLICAQKFNGLTVLPLLLTDEMI AQYTSALLAGTITSGWTFGAGAALQIPF	7V7Q_1 Chains	RASANLAATKMSCEVLGQSKRVDFCGKGYHLSMFPQSAHPGVVFLHVTYVPAQENFTTA
7T9J_1 Chains	DCLGDI AARDLICAQKFNGLTVLPLLLTDEMI AQYTSALLAGTITSGWTFGAGAALQIPF	7T9J_1 Chains	RASANLAATKMSCEVLGQSKRVDFCGKGYHLSMFPQSAHPGVVFLHVTYVPAQENFTTA
6VSB_1 Chains	DCLGDI AARDLICAQKFNGLTVLPLLLTDEMI AQYTSALLAGTITSGWTFGAGAALQIPF	6VSB_1 Chains	RASANLAATKMSCEVLGQSKRVDFCGKGYHLSMFPQSAHPGVVFLHVTYVPAQENFTTA
7VXD_1 Chains	DCLGDI AARDLICAQKFNGLTVLPLLLTDEMI AQYTSALLAGTITSGWTFGAGAALQIPF	7VXD_1 Chains	RASANLAATKMSCEVLGQSKRVDFCGKGYHLSMFPQSAHPGVVFLHVTYVPAQENFTTA
	***** * *****		***** * *****
7SBS_1 Chains	PAICHGDKAHFPRGQVFNSTGTHFVFTQNFYEPQIITDNTFVSGNCDVIGIVNNTVY	7SBS_1 Chains	DQSEPLVKGLKHYLLESGGGSAMSHQPEKGGGSGGSGGSSAMSHQPEK-----
7V7Q_1 Chains	PAICHGDKAHFPRGQVFNSTGTHFVFTQNFYEPQIITDNTFVSGNCDVIGIVNNTVY	7V7Q_1 Chains	KDGEWLLSTFLKQDN-----SAD-IQHSGR-----LESRPFQKLISEEDL
7T9J_1 Chains	PAICHGDKAHFPRGQVFNSTGTHFVFTQNFYEPQIITDNTFVSGNCDVIGIVNNTVY	7T9J_1 Chains	KDGEWLLSTFLGRSLE-----VL--FQGGHHHHHHHSHAWSHQPEKGGGSGGSGG
6VSB_1 Chains	PAICHGDKAHFPRGQVFNSTGTHFVFTQNFYEPQIITDNTFVSGNCDVIGIVNNTVY	6VSB_1 Chains	KDGEWLLSTFLGRSLE-----VL--FQGGHHHHHHHSHAWSHQPEKGGGSGGSGG
7VXD_1 Chains	PAICHGDKAHFPRGQVFNSTGTHFVFTQNFYEPQIITDNTFVSGNCDVIGIVNNTVY	7VXD_1 Chains	KDGEWLLSTFLLENL-----Y--FQGDYDDDDKHHHHHHHH-----
	***** * *****		***** * *****

with the ACE2. Used a wide-type spike glycoprotein interaction with ACE2 coded 6VW1 as a template. Table 1 and Figure 3 show the specific spike amino acid residues of the 6VW1 that interact with ACE2 amino acid residues. We observed no mutation in these interacting spike residues for the beta, delta, and gamma variants. For the omicron variant, which was studied using spike glycoprotein interaction with ACE2 coded 7WK6 as a template, we observed the introduction of different amino acid residues from its spike glycoprotein in interaction with ACE2, as shown in Table 1 and Figure 4. The implication is that a therapeutic intervention designed to obstruct the interaction of the viral spike protein with ACE2, based on the wide type variant, may fail in the omicron variant.

	PDB code: 6VW1		PDB code: 7WK6	
S/N	Spike	ACE2	Spike	ACE2
1	ASN 487	GLN 24, TYR 83	SER 494	HIS 34
2	GLN 493	GLU 35, LYS 31	ARG 493	GLU 35
3	ALA 475	SER 19	ASN 487	GLN 24, TYR 83
4	TYR 449	ASP38	TYR 489	TYR 83
5	TYR 505	GLU 37	THR 500	TYR 41
6	GLY 502	LYS 353	HIS 505	LYS 353
7	GLY 496	LYS 353	SER 496	LYS 353
8	THR 500	TYR 41	TYR 449	GLN 42
9	GLN 498	GLN 42	ARG 498	ASP 38, GLN 42

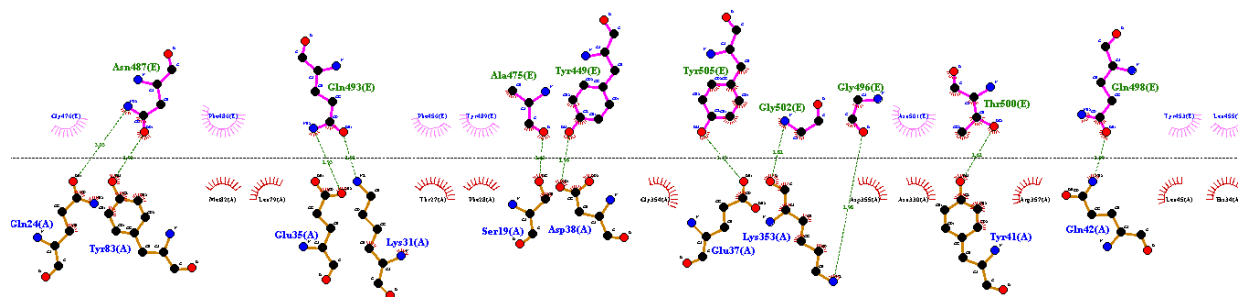


Figure 3: COVID-19 spike glycoprotein (wide-type; 6VW1) Interaction Bridge with ACE2 receptor

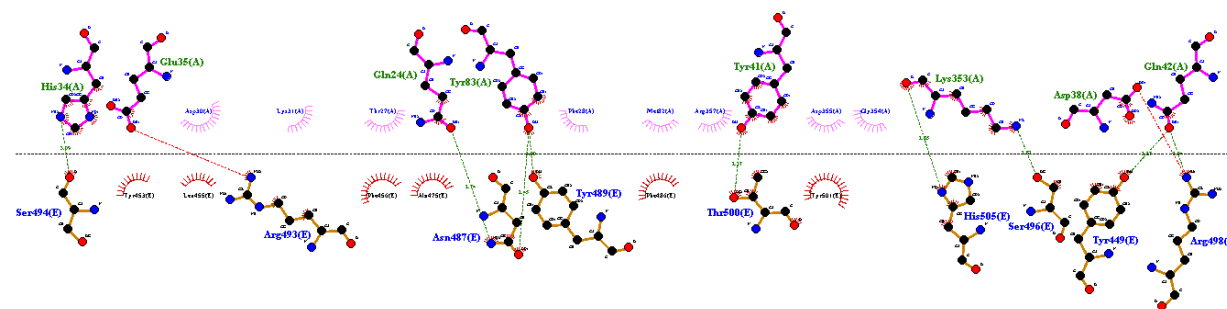


Figure 4: COVID-19 spike glycoprotein (Omicron; 7WK6) Interaction Bridge with ACE2 receptor

Molecular Docking Simulations and Post docking analysis

Moleculardocking simulation targeted four different points of spike glycoprotein and ACE2 interactions. The four interaction points were selected based on areas of similar amino acids for wide type and omicron variants. This is because, from the sequence alignment, the mutations observed were not located at the amino acid residue bridges between the spike glycoprotein and ACE2 in the wide-type, beta, delta and gamma variants. So, for the molecular docking simulations, we selected two points of interaction from the wide type TYR 449: ASP 38 and THR 500: TYR 41 (6VW1) and from omicron variant TYR 449: GLN 42 and THR 500: TYR 41 (7WK6).

The molecular docking results are presented in Tables 2, 3, 4 and 5. The results in the tables represent the top 20 drugs based on the mean values of binding affinities ranking.

Binding affinity and interaction analysis obtained by molecular docking help understand the molecular recognition in the drug-receptor complex. In computer-aided drug design, molecular docking is frequently used to forecast drug-protein complexes' preferred orientation and binding affinity. Protein-ligand docking predicts a ligand's preferred binding mode(s) with a target protein's three-dimensional structure [33].

From the rankings as presented in tables 2, 3, 4 and 5, we selected drugs that appeared at least in the three of the tables, and they include Dutasteride, Ergotamine, Folic acid, Piroxicam, Candesartan, Ketoconazole, Ceftriaxone, Amodiaquine, Methotrexate, Artesunate, Mebendazole, Bisacodyl and Tadalafil. Out of these, we selected eight drugs for visualization. The visualization will aid in understanding the interaction pattern between the drugs and the receptors: the spike glycoprotein and ACE2. The visualized drugs are Dutasteride, Ergotamine, Folic acid, Piroxicam, Ketoconazole, Ceftriaxone, Amodiaquine and Methotrexate.

Table 2: Binding affinities of the frontrunner drugs against 6VW1 point one interaction

S/N	Drug	Binding affinity 1	Binding affinity 2	Binding affinity 3	Mean	Standard deviation
1	Methotrexate	-7.50	-8.10	-8.20	-7.93	0.38
2	Tadalafil	-7.80	-7.80	-7.80	-7.80	0.00
3	Ergotamine	-7.50	-7.50	-7.80	-7.60	0.17
4	Mebendazole	-7.60	-7.60	-7.60	-7.60	0.00
5	Folic_Acid	-8.30	-7.10	-6.90	-7.43	0.76
6	Candesartan	-7.30	-7.30	-7.20	-7.27	0.06
7	Artesunate	-7.20	-7.30	-7.20	-7.23	0.06
8	Dutasteride	-7.10	-7.10	-7.10	-7.10	0.00
9	Bromocriptine	-7.00	-7.00	-7.00	-7.00	0.00
10	Ceftriaxone	-7.00	-7.00	-6.90	-6.97	0.06
11	Ketoconazole	-7.00	-6.90	-6.90	-6.93	0.06
12	Bisacodyl	-6.70	-6.90	-7.00	-6.87	0.15
13	Riboflavin	-6.80	-6.80	-6.80	-6.80	0.00
14	Amitriptyline	-6.60	-6.60	-6.60	-6.60	0.00
15	Lopinavir	-6.10	-6.00	-7.40	-6.50	0.78
16	Amoxicillin	-7.10	-6.10	-6.20	-6.47	0.55
17	Piroxicam	-6.40	-6.50	-6.50	-6.47	0.06
18	Sildenafil	-6.50	-6.40	-6.50	-6.47	0.06

19	Sulindac	-6.50	-6.50	-6.40	-6.47	0.06
20	Simvastatin	-6.40	-6.40	-6.50	-6.43	0.06

Table 3: Binding affinities of the frontrunner drugs against 6VW1 point two interaction

S/N	Drug	Binding affinity 1	Binding affinity 2	Binding affinity 3	Mean	Standard deviation
1	Meloxicam	-7.20	-7.20	-7.20	-7.20	0.00
2	Dutasteride	-7.00	-5.90	-7.60	-6.83	0.86
3	Ergotamine	-6.80	-6.80	-6.80	-6.80	0.00
4	Progesterone	-5.70	-6.90	-7.40	-6.67	0.87
5	Folic_Acid	-6.70	-6.50	-6.70	-6.63	0.12
6	Piroxicam	-6.40	-6.40	-6.40	-6.40	0.00
7	Sildenafil	-6.70	-5.40	-6.80	-6.30	0.78
8	Candesartan	-6.40	-6.40	-6.10	-6.30	0.17
9	Artesunate	-6.20	-6.40	-6.20	-6.27	0.12
10	Haloperidol	-6.40	-6.40	-6.00	-6.27	0.23
11	Ketoconazole	-6.00	-6.30	-6.30	-6.20	0.17
12	Methotrexate	-6.00	-6.60	-6.00	-6.20	0.35
13	Carbamazepine	-6.10	-6.10	-6.10	-6.10	0.00
14	Ampicillin	-6.10	-6.00	-6.00	-6.03	0.06
15	Dexamethasone	-6.40	-5.30	-6.40	-6.03	0.64
16	Tadalafil	-6.00	-6.00	-6.00	-6.00	0.00
17	Ceftriaxone	-6.20	-6.00	-5.70	-5.97	0.25
18	Quinine	-6.00	-5.90	-5.90	-5.93	0.06
19	Amodiaquine	-5.80	-5.90	-6.00	-5.90	0.10
20	Betamethasone	-5.90	-5.80	-5.90	-5.87	0.06

Table 4: Binding affinities of the frontrunner drugs against 7WK6 point one interaction

S/N	Drug	Binding affinity 1	Binding affinity 2	Binding affinity 3	Mean	Standard deviation
1	Dutasteride	-7.90	-8.10	-7.90	-7.97	0.12
2	Ketoconazole	-7.30	-7.40	-7.40	-7.37	0.06
3	Ergotamine	-7.50	-7.50	-7.00	-7.33	0.29
4	Bromocriptine	-7.30	-7.10	-7.30	-7.23	0.12
5	Candesartan	-7.30	-7.20	-7.20	-7.23	0.06
6	Tadalafil	-7.20	-7.20	-7.20	-7.20	0.00
7	Mebendazole	-7.20	-7.20	-7.10	-7.17	0.06
8	Losartan	-7.30	-6.80	-7.30	-7.13	0.29
9	Haloperidol	-7.10	-7.10	-6.90	-7.03	0.12
10	Amoxicillin	-6.80	-6.80	-6.80	-6.80	0.00
11	Folic_Acid	-6.80	-6.80	-6.70	-6.77	0.06
12	Lopinavir	-6.90	-6.90	-6.50	-6.77	0.23

13	Piroxicam	-6.70	-6.80	-6.80	-6.77	0.06
14	Loratadine	-6.70	-6.70	-6.80	-6.73	0.06
15	Ampicillin	-6.60	-6.60	-6.60	-6.60	0.00
16	Lorazepam	-6.50	-6.50	-6.50	-6.50	0.00
17	Morphine	-6.50	-6.50	-6.50	-6.50	0.00
18	Bisacodyl	-6.50	-6.50	-6.40	-6.47	0.06
19	Amitriptyline	-6.30	-6.50	-6.50	-6.43	0.12
20	Amodiaquine	-6.30	-6.30	-6.30	-6.30	0.00

Table 5: Binding affinities of the frontrunner drugs against 7WK6point two interaction

S/N	Drug	Binding affinity 1	Binding affinity 2	Binding affinity 3	Mean	Standard deviation
1	Artesunate	-7.30	-7.30	-7.20	-7.27	0.06
2	Tadalafil	-7.20	-7.20	-7.30	-7.23	0.06
3	Piroxicam	-7.00	-7.00	-7.00	-7.00	0.00
4	Mebendazole	-6.70	-6.60	-6.70	-6.67	0.06
5	Riboflavin	-6.30	-6.80	-6.90	-6.67	0.32
6	Folic_Acid	-6.20	-6.70	-6.80	-6.57	0.32
7	Methotrexate	-6.60	-6.70	-6.30	-6.53	0.21
8	Candesartan	-6.30	-6.60	-6.60	-6.50	0.17
9	Meloxicam	-6.50	-6.50	-6.50	-6.50	0.00
10	Quinine	-6.50	-6.50	-6.40	-6.47	0.06
11	Morphine	-6.40	-6.50	-6.40	-6.43	0.06
12	Bisacodyl	-6.30	-6.20	-6.20	-6.23	0.06
13	Carbamazepine	-6.20	-6.20	-6.20	-6.20	0.00
14	Ofloxacin	-6.20	-6.20	-6.20	-6.20	0.00
15	Oxycodone	-6.20	-6.20	-6.20	-6.20	0.00
16	Sulindac	-6.20	-6.20	-6.20	-6.20	0.00
17	Ceftriaxone	-6.30	-5.60	-6.30	-6.07	0.40
18	Amodiaquine	-6.10	-6.00	-6.00	-6.03	0.06
19	Levofloxacin	-6.00	-6.00	-6.00	-6.00	0.00
20	Prednisolone	-6.00	-6.00	-6.00	-6.00	0.00

2D visualization of the drug interaction with the receptors

Dutasteride shows a bridge of interaction between TYR 449 of the viral spike glycoprotein and ASP 38 of the ACE2 receptor, as shown in Figure 5a. This interaction is shown in Figure 3 as one of the interactions needed for the viral attachment to the ACE2 receptor. Dutasteride was able to bridge the interaction between TYR 449 and ASP 38, even though with a non-hydrogen bond, a hydrophobic bond.

Hydrophobic interactions affect how well medicines attach to their target proteins in drug-protein interactions. Research has indicated that hydrophobic interactions are crucial in determining a drug's affinity for particular protein binding sites [34]. These interactions may predominate at specific binding sites, impacting the drug's overall binding behaviour [34]. As shown in Figure 5b, Dutasteride interacted with hydrogen bonding to GLN 24 of ACE2, which was supposed to

form a bridge with ASN 487 of the viral spike glycoprotein. Drug actions are fundamentally influenced by hydrogen interactions, which impact several elements of drug design, stability, and efficacy. Drug-receptor interactions, binding affinity, and drug release kinetics are all affected by the hydrogen bonds generated between pharmaceuticals and other molecules, such as polymers or proteins [35,36]. According to Patil et al. (2010), these interactions are essential for changing binding affinities, stabilizing drug molecules at target sites, and improving treatment efficacy [35]. Robust interactions between drug and polymer hydrogen bonds enhance pharmaceuticals' physical and thermal stability during storage, preserve supersaturation upon dissolution, and improve drug processing. Furthermore, hydrogen bonding postpones drug crystallization in amorphous solid dispersions, enhancing drug dissolution performance [37]. Dutasteride also blocked the interaction between TYR 449 and GLN 42 using hydrophobic bonds, as shown in Figure 5c. It also interacted with HIS 34 using hydrogen bonds, which were supposed to form an interaction bridge with SER 494, as shown in Table 1 and Figure 4.

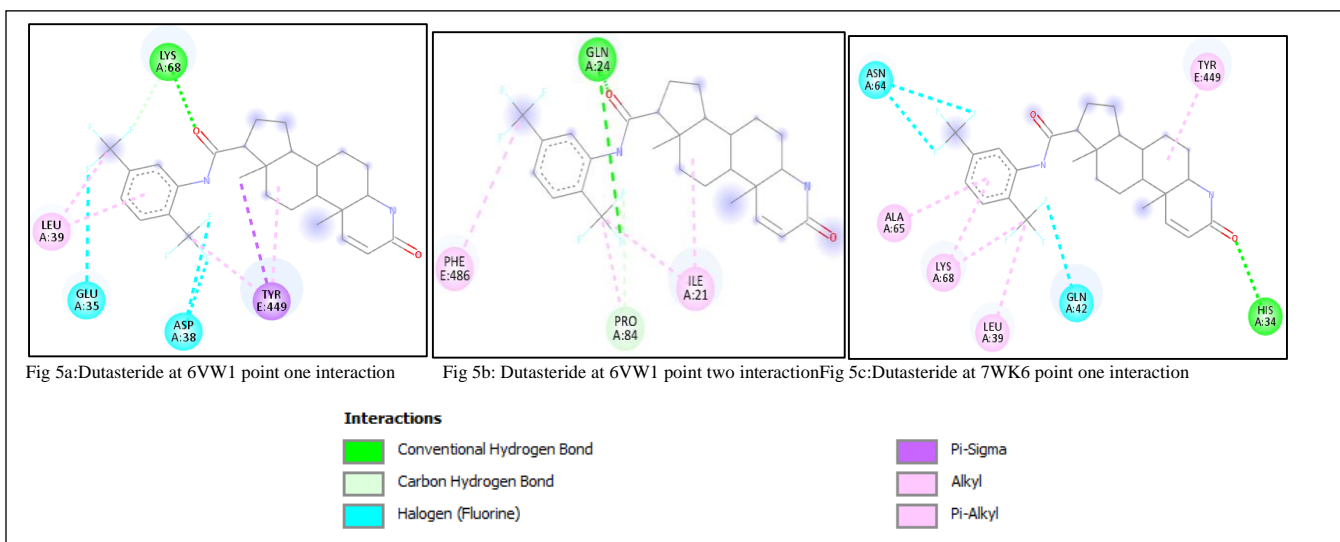
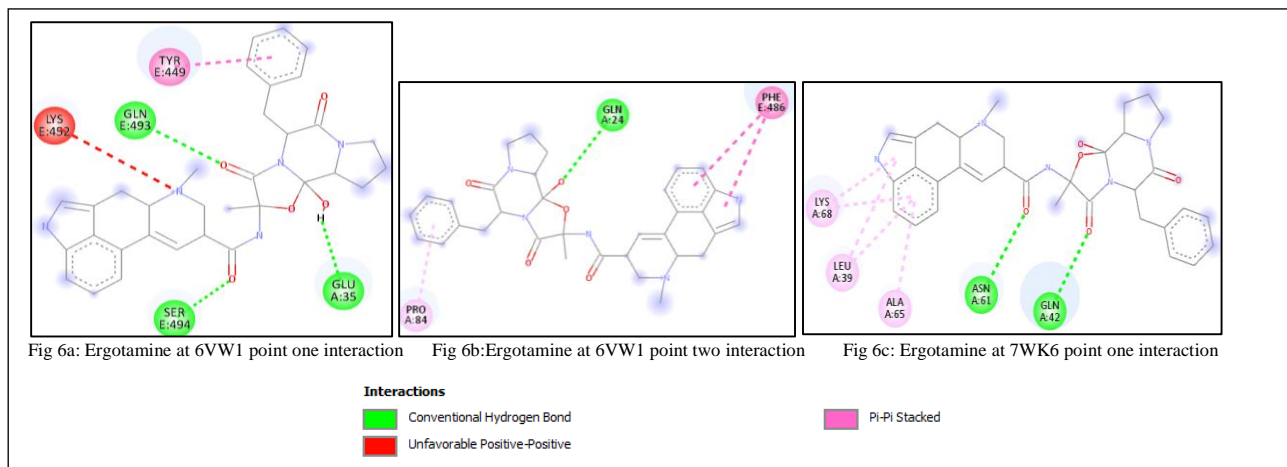
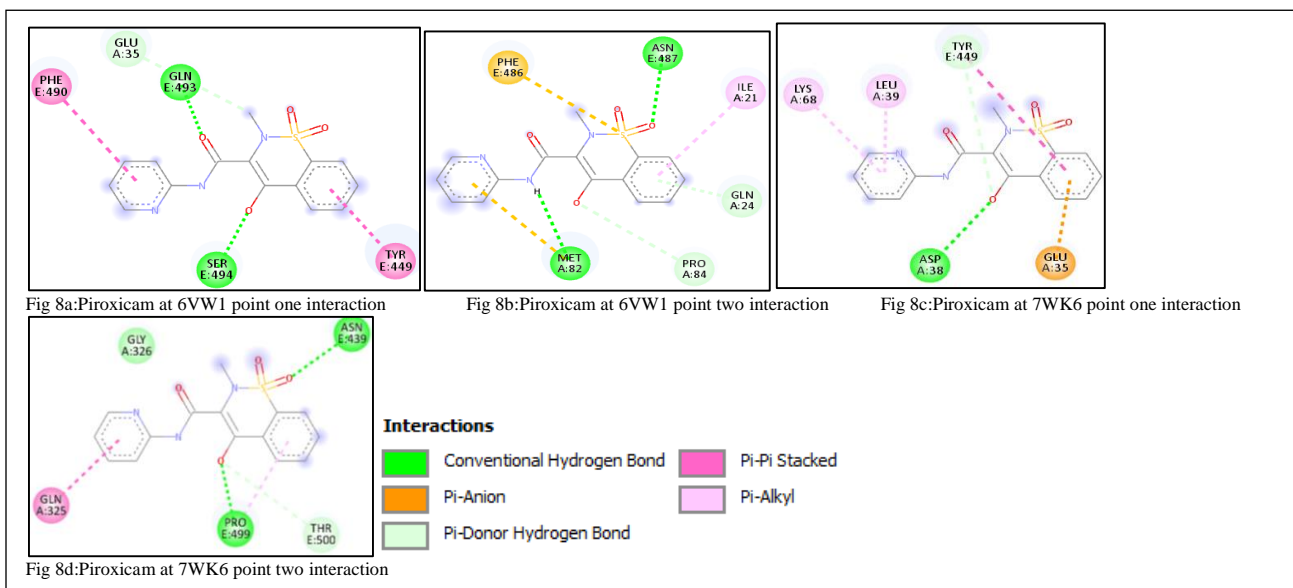
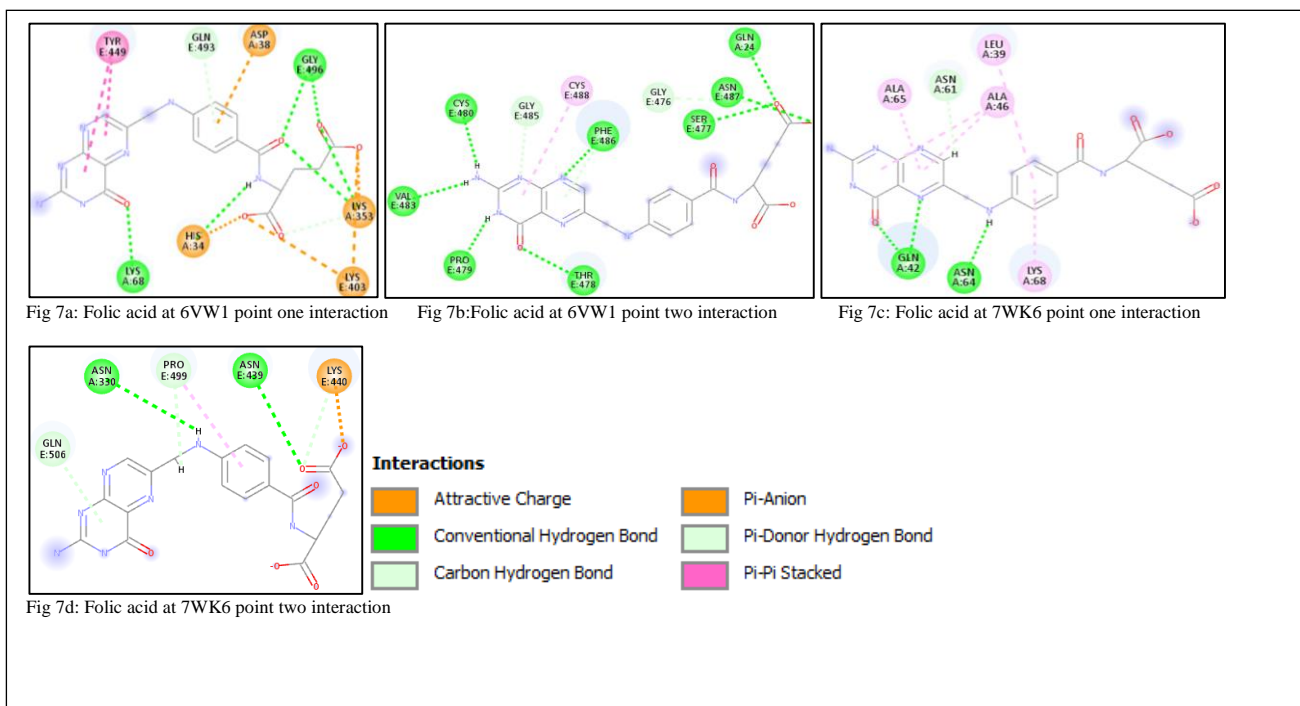


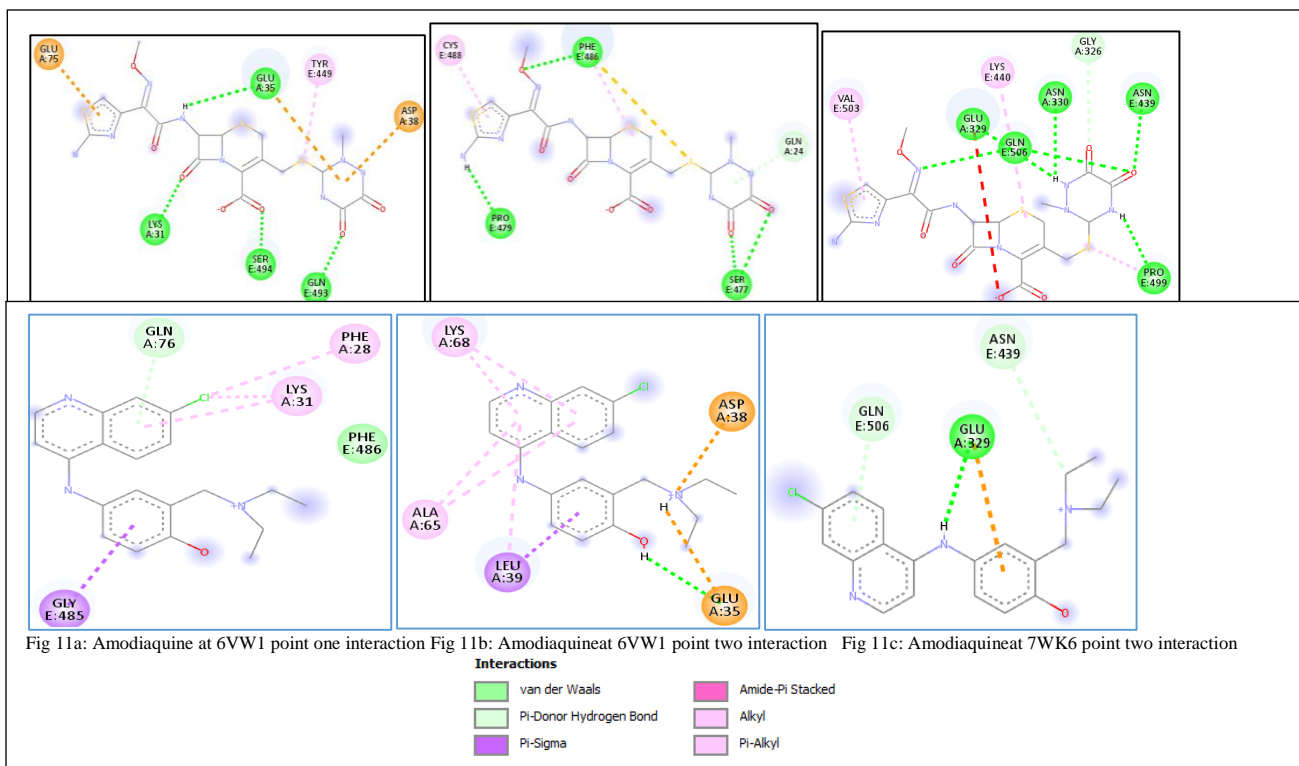
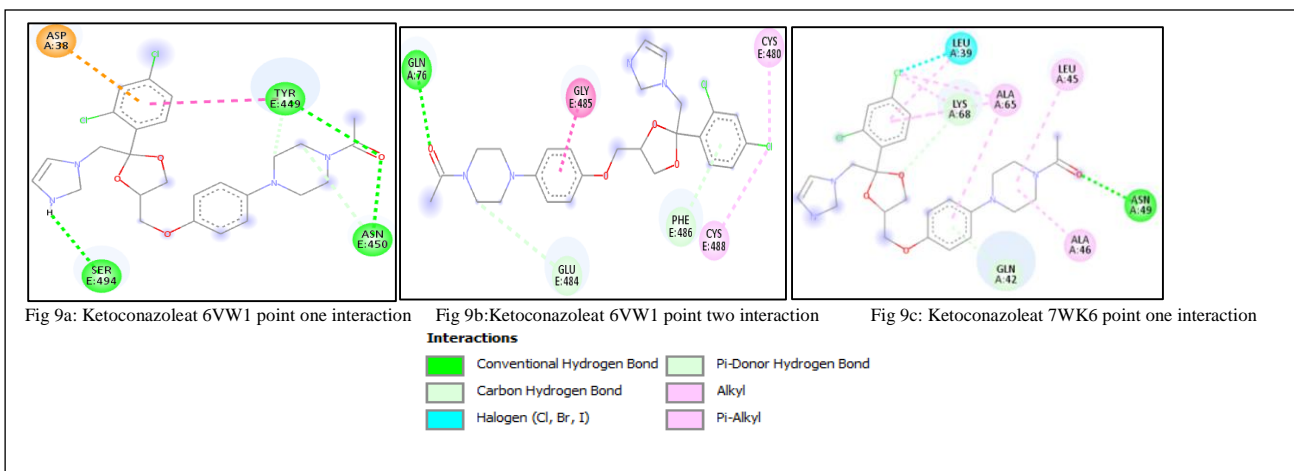
Figure 6b shows the establishment of hydrogen bond interaction between ergotamine and GLN 24 of ACE2. This GLN 24 is required for the interaction between the spike glycoprotein and the ACE2 receptor, as shown in Table 1 and Figure 3. Figure 6c also showed that ergotamine has hydrogen bond interaction with GLN 42 of the ACE2 receptor, which is required for bond formation with ASN 487 of the spike glycoprotein, as shown in Table 1 and Figure 4.

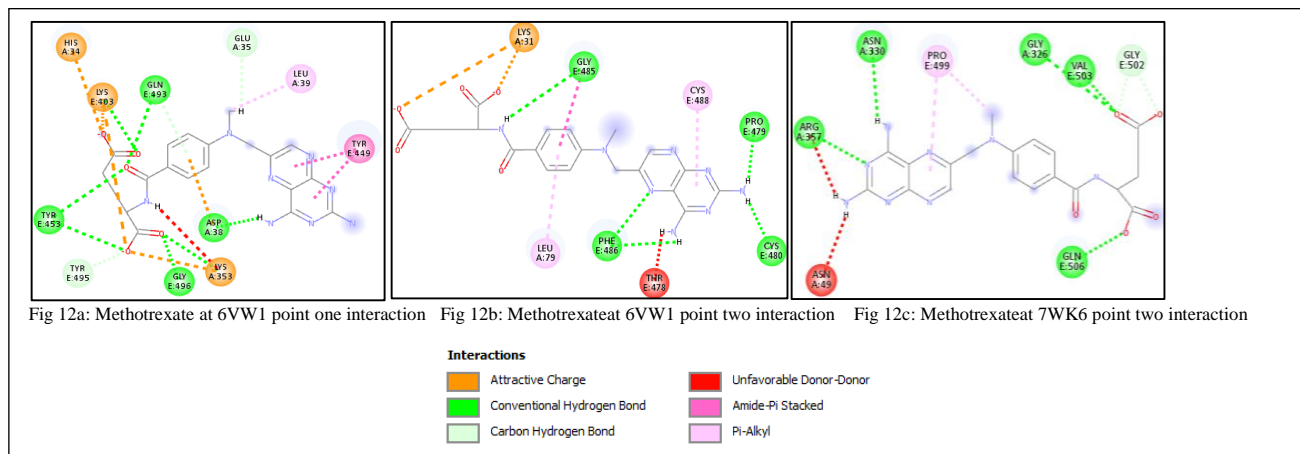


On the part of the ACE2 receptor for the 6VW1 point one interaction, folic acid exhibited some hydrophobic interactions with the amino acids of ACE2 required for interaction and bridge formation with the viral spike glycoprotein, as can be seen in Table 1, figure 3 and Figure 7a. At this point of interaction, folic acid also forms hydrogen interaction with GLN 496 of the viral spike glycoprotein. Figures 7b, 7c, and 7d show similar interaction obstructions of the amino acid of the spike glycoprotein and the host ACE2.

Figures 8a, 8b, 8c, and 8d show the interaction of Piroxicam with amino acids of the viral spike glycoprotein and ACE2. Figures 9a, 9b and 9c show the interactions of ketoconazole. Figures 10a, 10b, and 10c show interactions with ceftriaxone. Figures 11a, 11b, and 11c show interactions with amodiaquine. Figures 12a, 12b, and 12c show interactions with methotrexate.







This study and numerous other studies that impede the interaction between the COVID-19 spike glycoprotein and the ACE2 receptor have concentrated on developing inhibitors targeting this specific protein-protein interaction. The intention is to obstruct the binding of the SARS-CoV-2 spike protein to the ACE2 receptor, thereby impeding viral attachment and entry into host cells [38-41]. By disrupting this interaction, these inhibitors can be repurposed as antiviral agents against COVID-19 [39,40].

In-silico approaches have pinpointed compounds like propolis derivatives and N-ferrocenyl methyl derivatives that could efficiently inhibit the interaction between the spike glycoprotein and ACE2 [41,42]. These computational methods provide insights into the structural aspects of the spike glycoprotein and its binding to ACE2, aiding in formulating novel therapeutic strategies [41].

In the event of a pandemic in the future, studies of this nature can quickly be performed and validated to identify existing drug molecules and their derivatives that can help reduce mortality rates pending the development of a vaccine.

Conclusion

In this study, we observed the interaction of the approved drugs in the interaction bridges between spike COVID-19 spike glycoprotein and ACE2 receptor. We found that drug molecules can abridge the interaction between these two proteins. Further studies are required to understand the effects of the observed interaction and to check if the obstructions of the interactions observed can translate to inhibiting or delaying the viral attachment and entrance into host cells. We believe studies of this nature will provide insight on quick means of handling subsequent viral pandemic to avoid high mortality.

Reference

1. Wang D, Yin Y, Hu C, Liu X, Zhang X, Zhou S, Jian M, Xu H, Prowle J, Hu B, Li Y, Peng Z. Clinical course and outcome of 107 patients infected with the novel coronavirus, SARS-CoV-2, discharged from two hospitals in Wuhan, China. *Crit Care*. 2020 Apr 30;24(1):188
2. Muralidar, S., Ambi, S. V., Sekaran, S., & Krishnan, U. M. (2020). The emergence of COVID-19 as a global pandemic: Understanding the epidemiology, immune response and potential therapeutic targets of SARS-CoV-2. *Biochimie*, 179, 85–100.

3. COVID-19 Excess Mortality Collaborators (2022). Estimating excess mortality due to the COVID-19 pandemic: a systematic analysis of COVID-19-related mortality, 2020-21. *Lancet* (London, England), 399(10334), 1513–1536
4. Coronavirus cases by country in Africa 2022 | Statista. (2023, December 15). Statista. <https://www.statista.com/statistics/1170463/coronavirus-cases-in-africa/>
5. Choudhary, V., Gupta, A., Sharma, R., & Parmar, H. S. (2021). Therapeutically effective covalent spike protein inhibitors in treatment of SARS-CoV-2. *Journal of proteins and proteomics*, 12(4), 257–270.
6. Bai, C., Zhong, Q., & Gao, G. F. (2022). Overview of SARS-CoV-2 genome-encoded proteins. *Science China. Life sciences*, 65(2), 280–294.
7. Zhang, H., Penninger, J. M., Li, Y., Zhong, N., & Slutsky, A. S. (2020). Angiotensin-converting enzyme 2 (ACE2) as a SARS-CoV-2 receptor: molecular mechanisms and potential therapeutic target. *Intensive care medicine*, 46(4), 586–590.
8. Lee, Y. K., Chang, W. C., Prakash, E., Peng, Y. J., Tu, Z. J., Lin, C. H., Hsu, P. H., & Chang, C. F. (2022). Carbohydrate Ligands for COVID-19 Spike Proteins. *Viruses*, 14(2), 330.
9. Sanders JM, Monogue ML, Jodlowski TZ, Cutrell JB. Pharmacologic Treatments for Coronavirus Disease 2019 (COVID-19): A Review. *JAMA*. 2020 May 12;323(18):1824-1836
10. Laskowski R A, Swindells M B (2011). LigPlot+: multiple ligand-protein interaction diagrams for drug discovery. *J. Chem. Inf. Model.*, 51, 2778-2786
11. PyMOL. The PyMOL Molecular Graphics System, Version 3.0 Schrödinger, LLC.
12. Eberhardt, J., Santos-Martins, D., Tillack, A.F., Forli, S. (2021). AutoDock Vina 1.2.0: New Docking Methods, Expanded Force Field, and Python Bindings. *Journal of Chemical Information and Modeling*.
13. Trott, O., & Olson, A. J. (2010). AutoDock Vina: improving the speed and accuracy of docking with a new scoring function, efficient optimization, and multithreading. *Journal of computational chemistry*, 31(2), 455-461.
14. Biovia, D.S. (2019) Discovery Studio Visualizer. San Diego.
15. Li, F., Li, W., Farzan, M. & Harrison, S. C. [2005]. Structure of SARS coronavirus spike receptor-binding domain complexed with receptor. *Science* 309, 1864–1868
16. Li W, Moore MJ, Vasilieva N, Sui J, Wong SK, Berne MA, Somasundaran M, Sullivan JL, Luzuriaga K, Greenough TC, Choe H, Farzan M. Angiotensin-converting enzyme 2 is a functional receptor for the SARS coronavirus. *Nature*. 2003 Nov 27;426(6965):450-4
17. Shang J, Ye G, Shi K, Wan Y, Luo C, Aihara H, Geng Q, Auerbach A, Li F. Structural basis of receptor recognition by SARS-CoV-2. *Nature*. 2020 May;581(7807):221-224
18. Pirovano, W., & Heringa, J. (2008). Multiple sequence alignment. *Methods in molecular biology* (Clifton, N.J.), 452, 143–161
19. Tiede S, Cantz M, Spranger J, Bräulke T. (2006). Missense mutation in the N-acetylglucosamine-1-phosphotransferase gene (GNPTA) in a patient with mucopolysaccharidosis II induces changes in the size and cellular distribution of GNPTG. *Hum. Mutat*, 27:830–831.
20. Krumbholz M, Koehler K, Huebner A. (2006). Cellular localization of 17 natural mutant variants of ALADIN protein in triple A syndrome - shedding light on an unexpected splice mutation. *Biochem. Cell. Biol*, 84:243–249.

21. Yamada Y, Banno Y, Yoshida H, Kikuchi R, Akao Y, Murate T, Nozawa Y. (2006). Catalytic inactivation of human phospholipase D2 by a naturally occurring Gly901Asp mutation. *Arch. Med. Res*, 37:696–699.
22. Takamiya O, Seta M, Tanaka K, Ishida F. (2002). Human factor VII deficiency caused by S339C mutation located adjacent to the specificity pocket of the catalytic domain. *Clin. Lab. Haematol.* 24:233–238.
23. Jones R, Ruas M, Gregory F, Moulin S, Delia D, Manoukian S, Rowe J, Brookes S, Peters G. (2007). A CDKN2A mutation in familial melanoma that abrogates binding of p16INK4a to CDK4 but not CDK6. *Cancer Res*, 67:9134–9141.
24. Ung MU, Lu B, McCammon JA (2006). E230Q mutation of the catalytic subunit of cAMP-dependent protein kinase affects local structure and the binding of peptide inhibitor. *Biopolymers*, 81:428–439.
25. Rignall TR, Baker JO, McCarter SL, Adney WS, Vinzant TB, Decker SR, Himmel ME. (2002). Effect of single active-site cleft mutation on product specificity in a thermostable bacterial cellulase. *Appl. Biochem. Biotechnol*, 98–100:383–394.
26. Hardt M, Laine RA. (2004). Mutation of active site residues in the chitin-binding domain ChBDChiA1 from chitinase A1 of *Bacillus circulans* alters substrate specificity: use of a green fluorescent protein binding assay. *Arch. Biochem. Biophys*, 26:286–297.
27. Ode, H., Matsuyama, S., Hata, M., Neya, S., Kakizawa, J., Sugiura, W., Hoshino T. (2007). Computational characterization of structural role of the non-active site mutation M36I of human immunodeficiency virus type 1 protease. *J. Mol. Biol*, 370:598–607
28. Lorch, M., Mason, J.M., Sessions, R. B., Clarke, A. R. (2000). Effects of mutations on the thermodynamics of a protein folding reaction: implications for the mechanism of formation of the intermediate and transition states. *Biochemistry*, 39:3480–3485.
29. Lorch, M., Mason, J. M., Clarke, A. R., Parker, M. J. (1999). Effects of core mutations on the folding of a beta-sheet protein: implications for backbone organization in the I-state. *Biochemistry*, 38:1377–1385.
30. Alfalah, M., Keiser, M., Leeb, T., Zimmer, K. P., & Naim, H. Y. (2009). Compound heterozygous mutations affect protein folding and function in patients with congenital sucrase-isomaltase deficiency. *Gastroenterology*, 136(3), 883–892
31. Koukouritaki, S. B., Poch, M. T., Henderson, M. C., Siddens, L. K., Krueger, S. K., VanDyke, J. E., Williams, D. E., Pajewski, N. M., Wang, T., & Hines, R. N. (2007). Identification and functional analysis of common human flavin-containing monooxygenase 3 genetic variants. *The Journal of pharmacology and experimental therapeutics*, 320(1), 266–273
32. De Cristofaro, R., Carotti, A., Akhavan, S., Palla, R., Peyvandi, F., Altomare, C., & Mannucci, P. M. (2006). The natural mutation by deletion of Lys9 in the thrombin A-chain affects the pKa value of catalytic residues, the overall enzyme's stability and conformational transitions linked to Na⁺ binding. *The FEBS journal*, 273(1), 159–169
33. Morris, G. M., & Lim-Wilby, M. (2008). Molecular docking. *Methods in molecular biology* (Clifton, N.J.), 443, 365–382
34. Ranjbar, S., Shokoohinia, Y., Ghobadi, S., Bijari, N., Gholamzadeh, S., Moradi, N., ...& Khodarahmi, R. (2013). Studies of the interaction between isoimperatorin and human serum albumin by multispectroscopic method: identification of possible binding site of the compound using esterase activity of the protein. *The Scientific World Journal*, 2013, 1-13

35. Patil, R., Das, S., Stanley, A., Yadav, L., Sudhakar, A., &Varma, A. (2010). Optimized hydrophobic interactions and hydrogen bonding at the target-ligand interface leads the pathways of drug-designing. *Plos One*, 5(8), e12029.
36. Kothari, K., Ragoonanan, V., &Suryanarayanan, R. (2015). The role of drug-polymer hydrogen bonding interactions on nifedipine solid dispersions' molecular mobility and physical stability. *Molecular pharmaceutics*, 12(1), 162–170
37. Que, C., Deac, A., Zemlyanov, D. Y., Qi, Q., Indulkar, A. S., Gao, Y., Zhang, G. G. Z., & Taylor, L. S. (2021). Impact of Drug-Polymer Intermolecular Interactions on Dissolution Performance of Copovidone-Based Amorphous Solid Dispersions. *Molecular pharmaceutics*, 18(9), 3496–3508
38. Bojadzic, D., Garnica, Ó., Chen, J., Chuang, S., Capcha, J., Shehadeh, L., ... & Buchwald, P. (2021). Small-molecule inhibitors of the coronavirus spike: ace2 protein–protein interaction as blockers of viral attachment and entry for sars-cov-2. *Acs Infectious Diseases*, 7(6), 1519-1534.
39. Cao, L., Goreshnik, I., Coventry, B., Case, J., Miller, L., Kozodoy, L., ...& Baker, D. (2020). De novo design of picomolar sars-cov-2 miniprotein inhibitors. *Science*, 370(6515), 426-431
40. Sahlan, M., Dewi, L., Pratami, D., Lischer, K., &Hermansyah, H. (2023). In silico identification of propolis compounds potential as covid-19 drug candidates against sars-cov-2 spike protein. *International Journal of Technology*, 14(2), 387
41. Jafary, F., Jafari, S., &Ganjalkhany, M. R. (2021). In silico investigation of critical binding pattern in SARS-CoV-2 spike protein with angiotensin-converting enzyme 2. *Scientific reports*, 11(1), 6927
42. Zegheb, N., Elhafnaoui, L., &Lanez, T. (2020). N-ferrocenylmethyl-derivatives as spike glycoprotein inhibitors of sars-cov-2 using in silico approaches..<https://doi.org/10.26434/chemrxiv.12278078>